V European Conference on Computational Fluid Dynamics
ECCOMAS CFD 2010
J. C. F. Pereira and A. Sequeira (Eds)
Lisbon, Portugal,14-17 June 2010

COMPARISON OF ALGORITHMS FOR STRONGLY COUPLED PARTITIONED FLUID-STRUCTURE INTERACTION - EFFICIENCY VERSUS SIMPLICITY

Thomas Gallinger and Kai-Uwe Bletzinger

Lehrstuhl für Statik,
Technische Universität München,
Arcisstrasse 21, 80333 München
e-mail: {gallinger,kub}@bv.tum.de

Key words: Fluid-Structure Interaction, partitioned, strongly coupled, comparison of coupling algorithms, Aitken, quasi-Newton, Newton-Krylov, benchmark

Abstract. *In this paper, different common coupling algorithms for the partitioned simulation of strongly coupled fluid-structure interaction problems are compared. Typically, comparisons are made regarding efficiency and stability only, but here an additional emphasis is placed on the compatibility or necessity of adding extensions to the standard single field solution algorithms. The presented algorithms, which are compatible to standard field solution approaches are fixed-point iteration with Aitken-based relaxation and an incremental quasi-Newton method. Algorithms which are typically not compatible to standard solution approaches are Newton-Krylov methods. Here, two different approaches are analysed, namely finite-difference and linearized model evaluation of the Krylov space. The derivation of each algorithm is accompanied by a review regarding implementational aspects. Two numerical examples are used for comparison with respect to efficiency and stability.*

1 Introduction

The partitioned Dirichlet-Neumann approach is a very common solution method in the simulation of surface coupled problems. The main reason for this is the possibility to reuse existing single field solvers and to have great benefit from already exisiting solution approaches. Typically, one faces the problem that for a given or a desired combination of programs a coupling algorithm has to be chosen, which should combine high numerical efficiency and stability with low additional coding effort.

In this paper, the focus is on the simulation of strongly coupled problems with transient characteristic and large structural displacements. Different common coupling algorithms for this simulation type are compared, not only w.r.t. numerical efficiency and stability, but also w.r.t. necessary changes and adaptions to standard field solvers.

Examined coupling algorithms which allow the use of standard field solvers or black-box solvers are 1) Aitken's method as the most common approach, and 2) the quite recently developed quasi-Newton method of Vierendeels and Degroote. Newton-Krylov methods instead need additional evaluations of the Krylov space and are, therefore, typically not usable in combination with standard field solvers. However, they may show a remarkably higher efficiency. Finite-difference evaluation and linearized modeling of the Krylov space are examined.

This paper is organized as follows: In section 2 and 3, the field equations and solution approaches for the structure and the fluid field are introduced. In section 4, the coupled problem is formulated in an operator notation. In section 5, the different coupling algorithms are derived and an assessment concerning implementational aspects and the possibility of using black-box field solvers is made. Section 6 covers numerical investigations of the coupling algorithms including two different examples with differing coupling characteristics, examined w.r.t. numerical efficiency and stability. Based on these results a conclusion is drawn by evaluating the different algorithms.

2 Structure Field

The structure field is supposed to show a transient characteristic with large displacements. Therefore, as a solution approach, a geometricaly nonlinear formulation in combination with a time integration algorithm is chosen. The field is described by the momentum equation

$$\rho_S \frac{d^2\mathbf{d}}{dt^2} - \nabla \cdot (\mathbf{F} \cdot \mathbf{S}) = \mathbf{f} \quad in \quad \Omega^S, \tag{1}$$

and the constitutive and kinematic equations

$$\mathbf{S} = \mathbf{C} : \mathbf{E} \quad , \quad \mathbf{E} = \frac{1}{2}(\mathbf{F}^T \cdot \mathbf{F} - \mathbf{I}), \tag{2}$$

which give a relation between the second Piola-Kirchhoff stress $\mathbf{S}$, the Green-Lagrange strain $\mathbf{E}$, and the deformation gradient $\mathbf{F}$.

The Finite Element Method is used for discretization in space and the Generalized-α method[1] for discretization in time. This time integration method is implicit with second order accuracy and controllable numerical dissipation of high frequencies. Therefore, a combination of large structural time steps and high accuracy is possible. This leads to the following modified version of the general nonlinear equation of motion:

$$\mathbf{M} \cdot \ddot{\mathbf{d}}_\alpha + \mathbf{f}^{int}(\mathbf{d}_\alpha) = \mathbf{f}^{ext}_\alpha \tag{3}$$

with $\mathbf{M}$ the mass matrix, $\mathbf{f}^{int}$ the vector of internal forces, $\mathbf{f}^{ext}$ the vector of external forces, $\ddot{\mathbf{d}}$ the accelerations and $\mathbf{d}$ the displacements. Because

$$\begin{aligned} \ddot{\mathbf{d}}_\alpha = (1-\alpha_m)\ddot{\mathbf{d}}_{n+1} + \alpha_m \ddot{\mathbf{d}}_n \ , \ \mathbf{d}_\alpha = (1-\alpha_f)\mathbf{d}_{n+1} + \alpha_f \mathbf{d}_n \\ \mathbf{f}^{int}(\mathbf{d}_\alpha) \approx (1-\alpha_f)\mathbf{f}^{int}(\mathbf{d}_{n+1}) + \alpha_f \mathbf{f}^{int}(\mathbf{d}_n) \ , \ \mathbf{f}^{ext}_\alpha = (1-\alpha_f)\mathbf{f}_{ext,n+1} + \alpha_f \mathbf{f}_{ext,n} \end{aligned} \tag{4}$$

it can be seen that the Generalized-α method does not formulate the eqilibrium state at time $n+1$ (like e.g. Newmark-β method), but as a linear combination of the state at n and $n+1$ by using the shift-parameters α_m and α_f. Newmark's Ansatz[2] is used for the discretization of the state variables in time:

$$\begin{aligned} \mathbf{d}_{n+1} &= \mathbf{d}_n + \Delta t \dot{\mathbf{d}}_n + \frac{\Delta t^2}{2}(1-2\beta)\ddot{\mathbf{d}}_n + \beta \Delta t^2 \ddot{\mathbf{d}}_{n+1}, \\ \dot{\mathbf{d}}_{n+1} &= \dot{\mathbf{d}}_n + \Delta t(1-\gamma)\ddot{\mathbf{d}}_n + \gamma \Delta t \ddot{\mathbf{d}}_{n+1}. \end{aligned} \tag{5}$$

The combination of these methods leads to a system of equations which only unknown is the structural displacement $\mathbf{d}$ at time $n+1$. The fully discretized effective structure equation in its residual form is then given by

$$\begin{aligned} \mathbf{R}^S_{n+1}(\mathbf{d}_{n+1}) = M \cdot \left[(1-\alpha_m) \cdot \frac{1}{\beta \Delta t^2} \left(\mathbf{d}_{n+1} - \mathbf{d}_n - \Delta t \dot{\mathbf{d}}_n - \frac{\Delta t^2}{2}(1-2\beta)\ddot{\mathbf{d}}_n \right) + \alpha_m \cdot \ddot{\mathbf{d}}_n \right] \\ + (1-\alpha_f) \cdot \mathbf{f}^{int}_{n+1}\left(\mathbf{d}_{n+1}\right) + \alpha_f \cdot \mathbf{f}^{int}_n\left(\mathbf{d}_n\right) - (1-\alpha_f) \cdot \mathbf{f}^{ext}_{n+1} + \alpha_f \cdot \mathbf{f}^{ext}_n \end{aligned} \tag{6}$$

This is a nonlinear set of equations due to the contribution of the internal forces term.

Newton's method is used to solve this nonlinear problem iteratively. In every Newton iteration (iteration index i) the following linearized problem is solved:

$$\frac{\partial \mathbf{R}^{S,i}_{n+1}(\mathbf{d}^i_{n+1})}{\partial \mathbf{d}_{n+1}} \Delta \mathbf{d}^{i+1}_{n+1} = -\mathbf{R}^{S,i}_{n+1}(\mathbf{d}^i_{n+1}), \tag{7}$$

for the new displacement increment. The new displacement is given by

$$\mathbf{d}^{i+1}_{n+1} = \mathbf{d}^i_{n+1} + \Delta \mathbf{d}^{i+1}_{n+1}. \tag{8}$$

Newton iterations are stopped, if a certain convergence criterion is fulfilled, e.g.

$$\left| \mathbf{R}^{S,i+1}_{n+1}(\mathbf{d}^{i+1}_{n+1}) \right|_{L2} \leq \epsilon^S. \tag{9}$$

3 Fluid Field

The fluid field is supposed to show a transient characteristic on a time-varying domain with laminar flow. Therefore, the PISO-algorithm within an ALE-framework is chosen as the solution approach.

The fluid field is described by the incompressible form of the Navier-Stokes equations for Newtonian fluids, with the continuity and the momentum equations in their ALE form:

$$\begin{aligned} \nabla \cdot \mathbf{u} &= 0 \\ \frac{\partial \mathbf{u}}{\partial t} + (\mathbf{u} - \mathbf{u}_G) \nabla \mathbf{u} - \nabla \cdot (\nu \nabla \mathbf{u}) + \frac{1}{\rho} \nabla \mathbf{p} &= 0 \quad in \quad \Omega^F \end{aligned} \tag{10}$$

with $\mathbf{u}$ as the absolute velocity, $\mathbf{u_G}$ as the grid velocity and $\mathbf{p}$ as the pressure.

The Finite Volume Method is used for the discretization in space and the implicit second order backward differencing method for discretization in time[3,4], given by

$$\frac{\partial \mathbf{u}}{\partial t} = \frac{3\mathbf{u}^{n+1} - 4\mathbf{u}^n + \mathbf{u}^{n-1}}{2\Delta t}. \tag{11}$$

This nonlinear problem is solved by the PISO method[5,6] (Pressure Implicit with Split of Operators), which is an iterative method. It contains a predictor step, based on the linearized form of the momentum equation

$$\frac{\partial \mathbf{u}^P_{n+1}}{\partial t} + \phi_{rel,n} \nabla \mathbf{u}^P_{n+1} - \nabla \cdot \left(\nu \nabla \mathbf{u}^P_{n+1} \right) = -\frac{1}{\rho} \nabla \mathbf{p}_n, \tag{12}$$

giving an approximation of the new velocity field $\mathbf{u}^P_{n+1}$, and the PISO iterations (iteration index j). Every PISO iteration consists of two steps. First, the solution of the pressure equation, using the term $\tilde{\phi}$, which is based on the last known velocities,

$$\nabla \cdot \left(\frac{1}{a^j_p} \nabla \mathbf{p}^{j+1}_{n+1} \right) = \nabla \cdot \tilde{\phi}^j \tag{13}$$

and gives an estimate of the new pressure field $\mathbf{p}^{j+1}_{n+1}$. Second, the correction of the velocities w.r.t. the newly computed pressure. Typically, a predefined number of PISO iterations is executed, until convergence of the fluid equations is assumed and the continuity and momentum equations are fulfilled, i.e.

$$\left| \mathbf{R}^{F,j+1}_{n+1}(\mathbf{p}^{j+1}_{n+1}, \mathbf{u}^{j+1}_{n+1}) \right|_{L2} \leq \epsilon^F. \tag{14}$$

The variation of the fluid domain shape in time is modeled by using the relative fluxes ϕ_{rel} in the momentum equation. The connection between relative, absolute and grid fluxes is given by

$$\phi_{abs} = \phi_{rel} + \phi_G. \tag{15}$$

The grid fluxes ϕ_G are the result of the mesh motion algorithm. This algorithm adapts the fluid domain to the new shape with prescribed boundary positions and calculates the new position of the fluid nodes in the interior of the fluid domain. The mesh motion problem is defined as a Laplace problem on the fluid domain[7] with the node displacements $\mathbf{d}^F$ as unknowns:

$$\nabla \cdot (\gamma \nabla \mathbf{d}^F) = 0 \quad in \quad \Omega^F, \tag{16}$$

and prescribed boundary conditions:

$$\begin{aligned} \mathbf{d}^F &= \mathbf{d}^\Gamma \quad on \quad \Gamma, \\ \mathbf{d}^F &= 0 \quad on \quad \Gamma^F. \end{aligned} \tag{17}$$

γ is hereby an elementwise variable diffusion coeffienct, which influences the stiffness of the fluid mesh against deformation. It is typically defined depending on the minimal distance r_i between element centre and coupling interface Γ. Using quadratic inverse distance diffusicity leads to

$$\gamma_i(r_i) = \frac{1}{r_i^2}. \tag{18}$$

4 Coupling Conditions and Operator Formulation of the Coupled Problem

At the common interface between fluid and structure field Γ, certain conditions have to be fulfilled in order to establish equilibrium, which are the continuity of displacements and velocities

$$\mathbf{d}^{\Gamma_S} = \mathbf{d}^{\Gamma_F} \quad , \quad \dot{\mathbf{d}}^{\Gamma_S} = \mathbf{u}_G^{\Gamma_F}, \tag{19}$$

and the continuity of surface tension

$$n^{\Gamma_S} \cdot \tau^{\Gamma_S} = n^{\Gamma_F} \cdot \tau^{\Gamma_F}. \tag{20}$$

The solution of the coupled problem is based on a partitioned Dirichlet-Neumann approach. This means that the fluid and structure fields are solved as separate partitions and the interaction is captured by influencing the corresponding boundary conditions. For simplicity an operator notation is introduced[12], where the application of an operator means the solution of the corresponding field with a prescribed boundary value until full convergence.

The fluid field is solved for unknown velocities and pressures due to a given interface displacement $\mathbf{d}^\Gamma$, and is therefore the Dirichlet partition. The interface forces can be computed from the fluid solution. Its operator is denoted by $\mathcal{F}$ and its appliance gives:

$$\mathbf{f}^\Gamma = \mathcal{F}(\mathbf{d}^\Gamma). \tag{21}$$

The structure field is solved for unknown displacements due to prescribed boundary forces $\mathbf{f}^\Gamma$, and is therefore the Neumann partition. The interface displacements can be computed from the structure solution. Its operator is denoted by $\mathcal{S}$ and its appliance gives:

$$\tilde{\mathbf{d}}^{\Gamma} = \mathcal{S}(\mathbf{f}^{\Gamma}) = \mathcal{S}(\mathcal{F}(\mathbf{d}^{\Gamma})) = \mathcal{S} \circ \mathcal{F}(\mathbf{d}^{\Gamma}). \tag{22}$$

The interface displacements are the primal unknowns of the coupled problem, because the interface forces implicitly depend on them. Convergence of the coupled problem is reached, if the prescribed displacements $\mathbf{d}^{\Gamma}$ and the calculated displacements $\tilde{\mathbf{d}}^{\Gamma}$ match. Accordingly, the residuum at the interface is given by

$$\mathbf{R}^{\Gamma}(\mathbf{d}^{\Gamma}, \mathbf{f}^{\Gamma}) = \tilde{\mathbf{d}}^{\Gamma} - \mathbf{d}^{\Gamma} = \mathcal{S} \circ \mathcal{F}(\mathbf{d}^{\Gamma}) - \mathbf{d}^{\Gamma}. \tag{23}$$

A solution of the coupled problem is found, if the residua of the two fields and at the interface are below the corresponding tolerances:

$$\left|\mathbf{R}^{S}(\mathbf{d})\right|_{L2} \leq \epsilon^{S} \quad , \quad \left|\mathbf{R}^{F}(\mathbf{d}^{F}, \mathbf{u}, \mathbf{p})\right|_{L2} \leq \epsilon^{F} \quad , \quad \left|\mathbf{R}^{\Gamma}(\mathbf{d}^{\Gamma}, \mathbf{f}^{\Gamma})\right|_{L2} \leq \epsilon^{\Gamma}. \tag{24}$$

5 Coupling Algorithms for Strong Coupled Problems

If strong coupled problems are examined, the application of implicit coupling algorithms is necessary to obtain convergence of the coupled problem. In partitioned schemes, this implies an iterative solution of the problem (iteration index k), where in every iteration the interface displacements are prescribed and the fluid and structure field are solved to full convergence. The basic form of an implicit coupling algorithm is shown in algorithm 1.

It can be seen that in every coupling iteration the full solution of fluid and structure fields is necessary. This is the reason for the extensive numerical effort of implicit coupled computations. The most important part of the algorithm is the determination of the new interface displacement increment $\Delta\mathbf{d}_{n+1}^{\Gamma,k}$ in each iteration. For this task, the coupling algorithms introduced in the next sections use different approaches and techniques. Typically, the most important aspects in the comparison and evaluation of coupling algorithms are due to effectivity (necessary number of coupling iterations) and stability (convergence behavior and time step regularization). But an important reason for choosing a partitioned approach is quite often the possibility to reuse existing field solvers and their solution techniques. So an additional important factor is the compatibility of the coupling algorithm with standard single field solution approaches. Only if the algorithm shows superior efficiency and stability, this drawback maybe worthwhile.

In the next subsections, three common coupling algorithms suitable for strong coupled problems will be introduced and examined, also w.r.t. the possibility of reusing standard single field solution approaches. The comparison w.r.t. efficiency and stability is done in section 6.

5.1 Fixed-Point Iteration with Aitken Adaptive Underrelaxation

The basic form of any fixed-point method is given by

$$x^{k+1} = \Phi(x^{k}), \quad k = 1, ..., n, \tag{25}$$

Algorithm 1 Basic Form of an Implicit Dirichlet-Neumann Coupling Algorithm

for $t = 0$ to $t = t_{tot}$ **do**
  k=1
  while (!converged) **do**
    If(k==1) predict $\mathbf{d}_{n+1}^{\Gamma,k}$
    $\tilde{\mathbf{d}}_{n+1}^{\Gamma,k} = \mathcal{S} \circ \mathcal{F}(\mathbf{d}_{n+1}^{\Gamma,k})$
    $\mathbf{R}_{n+1}^{\Gamma,k} = \tilde{\mathbf{d}}_{n+1}^{\Gamma,k} - \mathbf{d}_{n+1}^{\Gamma,k}$
    if $\left(\left|\mathbf{R}_{n+1}^{\Gamma,k}\right|_{L2} < \epsilon^{\Gamma}\right)$ **then**
      $\mathbf{d}_{n+1}^{\Gamma} = \mathbf{d}_{n+1}^{\Gamma,k}$
      converged, go to next time step
    else
      $\Delta\mathbf{d}_{n+1}^{\Gamma,k} = f(\mathbf{R}_{n+1}^{\Gamma,k})$
      $\mathbf{d}_{n+1}^{\Gamma,k+1} = \mathbf{d}_{n+1}^{\Gamma,k} + \Delta\mathbf{d}_{n+1}^{\Gamma,k}$
    end if
    $k \leftarrow k + 1$
  end while
  $n \leftarrow n + 1$
end for

with the fixed-point operator Φ, giving a new solution of the problem based on the last solution. For surface coupled problems, at time $n+1$ the iteration directive reads

$$\Phi\left(\mathbf{d}_{n+1}^{\Gamma}\right) = \mathbf{d}_{n+1}^{\Gamma,k} + \Delta\mathbf{d}_{n+1}^{\Gamma,k}. \tag{26}$$

Using a relaxtion technique for the update of the interface displacement leads to

$$\begin{aligned}
\mathbf{d}_{n+1}^{\Gamma,k+1} &= \mathbf{d}_{n+1}^{\Gamma,k} + \Delta\mathbf{d}_{n+1}^{\Gamma,k} \\
&= \mathbf{d}_{n+1}^{\Gamma,k} + \omega^k \mathbf{R}_{n+1}^{\Gamma,k} \\
&= \mathbf{d}_{n+1}^{\Gamma,k} + \omega^k (\tilde{\mathbf{d}}_{n+1}^{\Gamma,k} - \mathbf{d}_{n+1}^{\Gamma,k}) \\
&= (1-\omega^k)\mathbf{d}_{n+1}^{\Gamma,k} + \omega^k \tilde{\mathbf{d}}_{n+1}^{\Gamma,k}
\end{aligned} \tag{27}$$

with ω^k as the relaxation factor in iteration k.

There exist different possibilities for the determination of ω, but the most efficient is Aitken's Δ^2-method[8,9,10]. As a basis, the Aitken factor has to be determined by

$$\mu_{n+1}^{k} = \mu_{n+1}^{k-1} + \left(\mu_{n+1}^{k-1} - 1\right) \frac{\left(\Delta\mathbf{d}_{n+1}^{\Gamma,k-1} - \Delta\mathbf{d}_{n+1}^{\Gamma,k}\right)^T \cdot \Delta\mathbf{d}_{n+1}^{\Gamma,k}}{\left(\Delta\mathbf{d}_{n+1}^{\Gamma,k-1} - \Delta\mathbf{d}_{n+1}^{\Gamma,k}\right)^2}, \tag{28}$$

with

$$\Delta \mathbf{d}_{n+1}^{\Gamma,k-1} = \tilde{\mathbf{d}}_{n+1}^{\Gamma,k-1} - \mathbf{d}_{n+1}^{\Gamma,k-1},$$
$$\Delta \mathbf{d}_{n+1}^{\Gamma,k} = \tilde{\mathbf{d}}_{n+1}^{\Gamma,k} - \mathbf{d}_{n+1}^{\Gamma,k}, \tag{29}$$

and the corresponding relaxation parameter is then given by

$$\omega^k = 1 - \mu_{n+1}^k. \tag{30}$$

Aitken's method is extremly easy to implement, because it just needs the evaluation of some vector products in each coupling step. Reuse of standard field solution approaches is guarenteed, because no additional information from the fields is needed and therefore black-box field solvers can be used. Due to these two reasons, Aitken's approach is the most commonly used method in the solution of strong coupled problems.

5.2 Quasi-Newton Method

The recently developed coupling algorithm of Vierendeels and Degroote[11,12,13] is a quasi-Newton method. Based on the change of the interface residual over coupling iterations, a minimization problem is solved and a new interface displacement increment is generated.

A starting procedure is needed to determine the first increments of residuum and displacement. For this, a prediction step followed by a constant relaxation step is performed. Then the quasi-Newton iterations are entered. The basic idea is that the desired interface residual in the next iteration should be zero: $\mathbf{R}^{\Gamma,k+1} = 0$. The desired change of the residual is therefore: $\Delta \mathbf{R}^k = 0 - \mathbf{R}^{\Gamma,k}$. This change is approximated by a linear combination of the known residual increments:

$$\Delta \mathbf{R}_{n+1}^{\Gamma,k} = 0 - \mathbf{R}_{n+1}^{\Gamma,k} \approx \sum_{i=1}^{k-1} \alpha_i^k \Delta \mathbf{R}_{n+1}^{\Gamma,i}. \tag{31}$$

This system is in general overdetermined and solved approximately as a minimization problem for the unknown linear coefficients α_i^k, e.g. with the least squares method:

$$\alpha^k = arg\, min \left|\left| \mathbf{R}_{n+1}^{\Gamma,k} + \sum_{i=1}^{k-1} \alpha_i^k \Delta \mathbf{R}_{n+1}^{\Gamma,i} \right|\right|_2. \tag{32}$$

The coefficients are now applied to the corresponding relaxed interface displacements

$$\Delta \tilde{\mathbf{d}}_{n+1}^{\Gamma,k} = \sum_{i=1}^{k-1} \alpha_i^k \Delta \tilde{\mathbf{d}}_{n+1}^{\Gamma,i}, \tag{33}$$

with $\Delta \tilde{\mathbf{d}}_{n+1}^{\Gamma,i} = \tilde{\mathbf{d}}^{\Gamma,i} - \tilde{\mathbf{d}}^{\Gamma,i-1}$. The correlation between $\mathbf{d}^\Gamma$ and $\tilde{\mathbf{d}}^\Gamma$ is given by $\mathbf{R}^\Gamma = \tilde{\mathbf{d}}^\Gamma - \mathbf{d}^\Gamma$, and therefore: $\mathbf{d}^\Gamma = \tilde{\mathbf{d}}^\Gamma - \mathbf{R}^\Gamma$. For the corresponding incremental state, this leads to

$$\Delta \mathbf{d}_{n+1}^{\Gamma,k} = \Delta \tilde{\mathbf{d}}_{n+1}^{\Gamma,k} - \Delta \mathbf{R}_{n+1}^{\Gamma,k} \tag{34}$$

for the determination of the new interface displacement increment.

This method allows the reuse of information from preceding coupling iterations to gain further speed-up of the coupling algorithm. The only thing to do is to add a series of preceding incremental residuum vectors to the minimization problem (32). This is possible, because for transient simulations it is expected that the relation between residual reduction and displacement increment is still valid to a certain extent in subsequent steps. An open question is how many preceding vectors have to be added to the minimization problem. This will be examined in section 6.

The quasi-Newton method presented here is more complicated to implement than Aitken's method. As the core requirement, the minimization problem has to be solved. The storage demand is also greater due to a major number of interface vectors which have to be stored. As with Aitken's method, standard black-box field solvers can be used because no additional information is needed from the fields.

5.3 Newton-Krylov Methods

Another popular group of methods for the solution of strongly coupled problems are Newton-Krylov methods. Newton methods are a standard solution approach for nonlinear problems and commonly used e.g. in structural and fluid mechanics. Using Newton-methods for the solution of coupled problems is therefore a natural choice, but the specific characteristics of coupled problems do not allow the use of standard procedures.

Newton methods are iterative methods, which solve in each iteration a linearized problem. For coupled problems, this reads:

$$\frac{\partial \mathbf{R}_{n+1}^{\Gamma,k}}{\partial \mathbf{d}^{\Gamma}} \Delta \mathbf{d}_{n+1}^{\Gamma,k} = -\mathbf{R}_{n+1}^{\Gamma,k} \tag{35}$$

with $\mathbf{R}^{\Gamma}$ as the interface residual and $\frac{\partial \mathbf{R}^{\Gamma}}{\partial \mathbf{d}^{\Gamma}}$ as the interface Jacobian, which is the linearization of the nonlinear coupled problem at the current position $\mathbf{d}^{\Gamma}$. For the general case of nonlinear field solvers it is not possible to evaluate the Jacobian directly. But there exists a variety of approaches which are based on an approximation of the Jacobian matrix. A common way in coupled problems is to use a Krylov solver, i.e. GMRES, for the solution of eqn. (35). Krylov solvers find solutions for linear systems of equations by evaluating the Krylov space of the problem and minimizing the equation residual over this space[14]. The advantage of Krylov methods within the context of coupled problems is, that the Jacobian matrix is not needed explicitly, but only the evaluation of the matrix times the Krylov vectors.

A coupling algorithm based on Newton-Krylov methods is shown in algorithm 2. It can be seen, that in every coupling iteration the current tangent problem is solved by additional iterations to evaluate the Krylov space (iteration index m). The GMRES algorithm is used to calculate the new Krylov vector $\mathbf{v}_{m+1}$. As the input the Krylov space evaluation corresponding to $\mathbf{v}_m$ is needed, which means that the term

$$\frac{\partial \mathbf{R}_{n+1}^{\Gamma,k}}{\partial \mathbf{d}^{\Gamma}} \mathbf{v}_m \tag{36}$$

has to be evaluated in every GMRES iteration. Because the Jacobian is not known, only an approximation is possible. The approximation of this matrix-vector product is the key ingredient of all Newton-Krylov coupling algorithms, as the relation between quality of the approximation and numerical effort has the decisive influence to the efficiency of the whole method.

After the tangent problem is solved by GMRES until convergence, the new interface displacement increment is given as a linear combination of the Krylov vectors

$$\Delta \mathbf{d}_{n+1}^{\Gamma,k+1} = \sum_{n=1}^{m} \mathbf{v}_n \alpha_n, \tag{37}$$

with the linear coefficients α_n as the solution of the corresponding minimization problem

$$\alpha_n = arg\, min \left|\left| \mathbf{R}_{n+1}^{\Gamma,k} - \sum_{n=1}^{m} \alpha_n \left(\mathbf{R}_{n+1}^{\Gamma,k} \right)' \mathbf{v}_n \right|\right|_2 . \tag{38}$$

In the subsequent section, two different methods of Krylov space evaluation are introduced. The evaluation of the coupled problem over the Krylov space is performed by specific Krylov field operators marked by a star, so $\mathcal{F}^{\star}$ for the specific fluid field and $\mathcal{S}^{\star}$ for the specific structure field.

5.3.1 Krylov-Space Evaluation by Finite Differences

A very simple way to evaluate the Krylov space is to use global Finite Differences[15,16,17,18]. Using e.g. a first order approximation the matrix-vector product is given by

$$\frac{\partial \mathbf{R}_{n+1}^{\Gamma,k}(\mathbf{d}_{n+1}^{\Gamma,k})}{\partial \mathbf{d}^{\Gamma}} \mathbf{v}_m \approx \frac{\mathbf{R}_{n+1}^{\Gamma,k}(\mathbf{d}_{n+1}^{\Gamma,k} + \alpha \mathbf{v}_m) - \mathbf{R}_{n+1}^{\Gamma,k}(\mathbf{d}_{n+1}^{\Gamma,k})}{\alpha}. \tag{39}$$

The interface residual $\mathbf{R}_{n+1}^{\Gamma,k}$ is already known and the residual at $\mathbf{R}_{n+1}^{\Gamma,k}(\mathbf{d}_{n+1}^{\Gamma,k} + \alpha \mathbf{v}_m)$ can be evaluated by using the standard field operators $\mathcal{F}$ and $\mathcal{S}$. The specific field operators $\mathcal{F}^{\star}$ and $\mathcal{S}^{\star}$ are therefore identical with the standard field operators, which have to be evaluated at the position $\mathbf{d}_{n+1}^{\Gamma,k} + \alpha \mathbf{v}_m$, leading to

$$\mathbf{R}_{n+1}^{\Gamma,k}(\mathbf{d}_{n+1}^{\Gamma,k} + \alpha \mathbf{v}_m) = \mathcal{S} \circ \mathcal{F}(\mathbf{d}_{n+1}^{\Gamma,k} + \alpha \mathbf{v}_m) - (\mathbf{d}_{n+1}^{\Gamma,k} + \alpha \mathbf{v}_m). \tag{40}$$

By definition, the Krylov vectors are of length one. Therefore, the scalar α is used to scale the Krylov vectors and evaluate the response of the coupled problem within a meaningful radius. The choice of α has a major influence on the evaluation quality.

A Finite Difference based evaluation of the Krylov space has the advantage, that the standard problem is evaluated. Therefore, standard field solvers can be used and even

Algorithm 2 Newton-Krylov Coupling Algorithm

for $t = 0$ to $t = t_{tot}$ **do**
  k=1
  while (!coupling convergence) **do**
    If(k==1) predict $\mathbf{d}_{n+1}^{\Gamma,k}$
    $\tilde{\mathbf{d}}_{n+1}^{\Gamma,k} = \mathcal{S} \circ \mathcal{F}(\mathbf{d}_{n+1}^{\Gamma,k})$
    $\mathbf{R}_{n+1}^{\Gamma,k} = \tilde{\mathbf{d}}_{n+1}^{\Gamma,k} - \mathbf{d}_{n+1}^{\Gamma,k}$
    if $\left(\left|\mathbf{R}_{n+1}^{\Gamma,k}\right|_{L2} < \epsilon^{\Gamma}\right)$ **then**
      $\mathbf{d}_{n+1}^{\Gamma} = \mathbf{d}_{n+1}^{\Gamma,k}$
      coupling converged, go to next time step
    else
      Evaluate Krylov space:
      $\mathbf{v}_1 = \mathbf{R}_{n+1}^{\Gamma,k} / \left|\left|\mathbf{R}_{n+1}^{\Gamma,k}\right|\right|_2$
      $m = 1$
      while (!GMRES convergence) **do**
        $(\mathbf{R}_{n+1}^{\Gamma,k})' \mathbf{v}_m = f(\mathcal{S}^{\star} \circ \mathcal{F}^{\star}(\mathbf{v}_m))$
        $\mathbf{v}_{m+1} = GMRES \rightarrow f((\mathbf{R}_{n+1}^{\Gamma,k})' \mathbf{v}_m)$
        if $\left(\left|\mathbf{R}_{n+1}^{\Gamma,k} - \sum_{n=1}^{m} \alpha_n \left(\mathbf{R}_{n+1}^{\Gamma,k}\right)' \mathbf{v}_n\right|_{L2} \leq \epsilon^{K}\right)$ **then**
          $\Delta \mathbf{d}_{n+1}^{\Gamma,k+1} = \sum_{n=1}^{m} \mathbf{v}_n \alpha_n$
          $\mathbf{d}_{n+1}^{\Gamma,k+1} = \mathbf{d}_{n+1}^{\Gamma,k} + \Delta \mathbf{d}_{n+1}^{\Gamma,k}$
          GMRES converged, go to next coupling step
        else
          $m \leftarrow m + 1$
        end if
      end while
    end if
    $k \leftarrow k + 1$
  end while
  $n \leftarrow n + 1$
end for

the usage of black-box solvers is possible. Additionally, for the optimal choice of α the evaluation quality is very high, because the complete problem is evaluated. Nevertheless, this method has three major disadvantages:

- The influence of α on the quality of the evaluation is great, but guidelines for its determination are rather unknown. For large values of α, the field solvers will not converge, and for very small values of α, numerical rounding errors will have great influence.
- In every coupling iteration, additional multiple solutions of the whole problem are necessary. This leads to high additional numerical effort.
- Due to the orthogonality of the Krylov vectors, the additional field solutions can be more expensive than the standard solutions, because there's no continuous convergence against the final result.

5.3.2 Krylov-Space Evaluation by Linearized Model

Another common method of Krylov space evaluation is to use a simplified model, in which the physics of the problem is maintained, but the nonlinearities of both fields and the fluid domain adaption are neglected[19,21]. This is called a linearized model and is based on the assumption, that a linearization at the current state gives enough information for a qualitative evaluation.

The fluid domain is frozen arround the current state $\Omega^{F,k}_{n+1}$, and an Eulerian fluid model is used. The Krylov vector is used as a bondary condition for fluxes and velocities by transformation into a boundary velocity. All other boundary conditions are identical to the full model. The velocity predictor step is skipped and only one iteration of the PISO loop is executed. The specific fluid field operation $\mathbf{f}^{\star}_{m+1} = \mathcal{F}^{\star}(\mathbf{v}_m)$ is given by:

$$\begin{aligned}
\nabla \cdot \left(\frac{1}{a_p^j} \nabla \mathbf{p}^{\star,m+1}_{n+1} \right) &= \nabla \cdot \tilde{\phi}^{\star,k} \qquad in \quad \Omega^{F,k}_{n+1}, \\
\mathbf{p}^{\star,m+1}_{n+1} &= \mathbf{p}^{k}_{n+1} \qquad on \quad \Gamma^{F,k}_{n+1}, \\
\mathbf{u}^{\star,m+1}_{n+1} &= \mathbf{u}^{k}_{n+1} \qquad on \quad \Gamma^{F,k}_{n+1}, \\
\mathbf{u}^{\star,m+1}_{n+1} &= \frac{\mathbf{v}_m}{\Delta t} \qquad on \quad \Gamma^{FSI,k}_{n+1}.
\end{aligned} \tag{41}$$

On the structure field, the current tangential effective stiffness matrix is evaluated. The specific structure field operation $\tilde{\mathbf{v}}_{m+1} = \mathcal{S}^{\star}(\mathbf{f}^{\star}_{m+1})$ is therefore given as:

$$\frac{\partial \mathbf{R}^{k}_{S,n+1}(\mathbf{d}^{k}_{n+1})}{\partial \mathbf{d}_{n+1}} \tilde{\mathbf{v}}_{m+1} = \mathbf{f}^{\star}_{m+1} \qquad in \quad \Omega^{S,k}_{n+1}. \tag{42}$$

The matrix-vector product can then be evaluated by:

$$\frac{\partial \mathbf{R}_{n+1}^{\Gamma,k}(\mathbf{d}_{n+1}^{\Gamma,k})}{\partial \mathbf{d}^{\Gamma}}\mathbf{v}_m = \mathbf{v}_m - \tilde{\mathbf{v}}_{m+1} \tag{43}$$

This approach has the advantage, that all relevant physical flow quantities can be captured and the numerical effort for the evaluation is low. Only two linear systems have to be solved in each Krylov iteration. There are mainly three disadvantages to state:

1. Neglecting the mesh motion leads to wrong matrix coefficients in the equation systems and the interface is no longer a wall boundary. The effect of these errors is strongly problem dependend.

2. The evaluation quality due to linearization is good, only if the nonlinear effects are comparably small. Therefore, time step size and coupling degree have strong influence.

3. Because simplified models have to be setup in the field solvers, the usage of black-box field solvers is no longer possible.

6 Numerical Investigation

In this section the above-mentioned coupling algorithms are compared w.r.t. numerical efficiency and stability. As an example, the cases FSI2 and FSI3 of the model problem introduced by Turek and Hron[22] are chosen, because of having the following properties: 1) These cases show transient behavior with large displacements and are strongly coupled. 2) Exact definitions of geometry and physical quantities are given and the single field models are simple. 3) There exist results from different groups[23,24], so that the reference values are expected to be verified.

The geometry of both cases is the same and only the physical quantities are changed. A sketch of the computational domain is given in fig. 1. The rectangular fluid domain has a parabolic inlet on the left, an outlet on the right and walls on top and bottom. A rigid cylinder is placed slightly asymmetric within the domain and an elastic beam is attached to the back of the cylinder. The length is $2.5\,[m]$, height is $0.41\,[m]$, the cylinder center is at $(0.2, 0.2\,[m])$ with a radius of $0.05\,[m]$. The elastic beam has the length of $0.6\,[m]$ and height of $0.02\,[m]$. The physical quantities of the two cases are summarized in table 1. A more detailed descripion is given e.g. in Turek(2006).

	$\frac{\rho^S}{\rho^F}$	$\rho^S\ \left[\frac{kg}{m^3}\right]$	$\nu^S\,[-]$	$E\ \left[\frac{kg}{m^3}\right]$	$\rho^F\ \left[\frac{kg}{m^3}\right]$	$\nu^F\ [-]$	$U_{max}\ \left[\frac{m}{s}\right]$	$Re\,[-]$
FSI2	10.0	10000	0.4	$1.4e^{06}$	1000	$1e^{-03}$	1.5	100
FSI3	1.0	1000	0.4	$5.6e^{06}$	1000	$1e^{-03}$	3	200

Table 1: Physical parameters for FSI2 and FSI3

The laminar fluid field is modeled using an implicit 2nd order Finite Volume Method on a structured grid. The structure field is modeled as a cantilever beam using an implicit

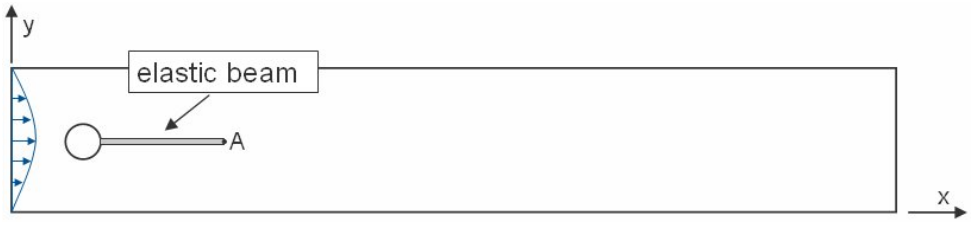

Figure 1: Computational domain

2nd order Finite Element Method with shell elements. Every coupling algorithm starts with a predictor of the interface displacements. Here, a 1st order Newmark-type predictor is used in all methods, given by $\mathbf{d}_{n+1}^{\Gamma,P} = \mathbf{d}_n^{\Gamma} + \Delta t \dot{\mathbf{d}}_n^{\Gamma}$. The usage of this predictor leads to an inital relative residual in the order of 10^{-1} in the first coupling iteration. The coupling algorithms compared are Aitken's method (FPA), Quasi-Newton method without (QN) and with reuse (QN-R) of information, Newton-Krylov method with finite differences (NKFD) and linearized problem modeling (NKLP), also without and with reuse of Krylov vectors (NKFD-R and NKLP-R). For reuse of information 10 and 20 history levels are taken into account. For the Krylov methods the numbers in brackets denote the average number of additional Krylov iterations per time step. In NKFD the scaling factor α is set to $\alpha = 1.0e^{-4}$. This is the result of a comparative study giving best performance. The coupling iterations are converged, if a relative convergence criteria of $\epsilon^{\Gamma} \leq 10^{-5}$ is fulfilled, which is a comparably demanding value.

6.1 Problem FSI2

The resulting transient displacement of point A in x- and y-direction is shown in fig. 2. It can be seen, that after an inital phase, the beam shows a harmonic oscillation with constant frequency and amplitude, which is the result of the interaction between Karmann vortices and beam displacement.

In the following, the different coupling algorithms are used to compute the coupled system's behavior. The first 500 timesteps are computed. To compare w.r.t. efficiency, the average number of necessary coupling iterations and the relative computing time is given. To compare w.r.t. stability, two increasing time step sizes are examined, $\Delta t = 5.0e^{-4}\,[s]$, what corresponds to a maximum Courant number of 0.8, and $\Delta t = 10.0e^{-4}\,[s]$, what corresponds to a maximum Courant number of 1.6, in the undeformed fluid configuration. The results are summarized in table 2.

As the standard approach, Aitken's method (**FPA**) needs 8.984 iterations with $\Delta t = 5.0e^{-4}\,[s]$ and 9.348 iterations with $\Delta t = 10.0e^{-4}\,[s]$, so the influence of the larger time step is quite small. The Quasi-Newton method in its basic version (**QN**) only needs 5.356 and 5.964 iterations, so a reduction of -40.4% and -36.2% is obtained. Again, the influence of the larger time step is quite small. Because the convergence criteria is given by $\epsilon^{\Gamma} \leq 10^{-5}$ the basic QN method yields approximately linear convergence. Reuse

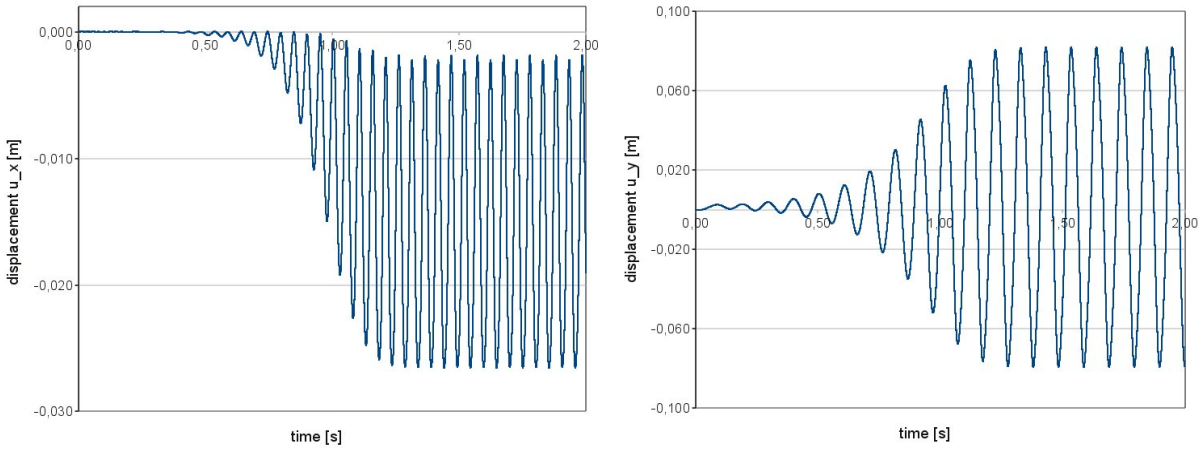

Figure 2: FSI2 - Displacement of Point A in x- and y-direction

	$\Delta t = 0.0005$		$\Delta t = 0.001$	
	Iterations	CPU time	Iterations	CPU time
FPA	8.984	1.00	9.348	1.00
QN	5.356	0.62	5.964	0.67
QN-R(10)	3.562	0.40	4.926	0.53
QN-R(20)	3.470	0.39	4.904	0.52
NKFD	5.126 (11.146)	2.23	5.262 (14.668)	2.58
NKFD-R(10)	5.006 (6.404)	1.55	5.248 (7.490)	1.67
NKFD-R(20)	5.012 (5.116)	1.34	5.248 (6.218)	1.52
NKLP	5.612 (12.320)	0.94	5.020 (12.762)	0.84
NKLP-R(10)	5.604 (6.182)	0.76	5.020 (6.85)	0.68
NKLP-R(20)	5.604 (5.450)	0.71	5.022 (5.58)	0.65

Table 2: Comparison for FSI2

of history information (**QN-R**) gives an additional large increase in performance with low additional cost. Reusing 20 history levels (QN-R(20)) leads to 3.47 iterations with $\Delta t = 5.0e^{-4}\,[s]$ and a reduction of -35.2% and 4.90 iterations with $\Delta t = 10.0e^{-4}\,[s]$ and a reduction of -17.8% compared to QN. Here, a larger influence of the time step size can be observed. This is as expected, because the information quality of preceding time steps decreases for larger time steps. Newton-Krylov with Finite Differences (**NKFD**) need a little bit more than 5 iterations. NKFD is therefore slightly better then QN in terms of total iterations and gives approximately linear convergence rates. Reuse of Krylov information (**NKFD-R**) leads to a significant reduction of necessary GMRES iterations (-54.1% for $\Delta t = 5.0e^{-4}\,[s]$ and -57.6% for $\Delta t = 10.0e^{-4}\,[s]$). The number of coupling iterations remains constant, because the solution tolerance of eqn. (40) is not influenced by the reuse. It is important to note, that every Krylov iteration has approximately the

same cost as one coupling iteration. So to compare NKFD with other schemes, the CPU time is a better evaluation criteria. Here, it can be seen that NKFD needs 2.23 and 2.58 times more CPU time than FPA, and even reuse of 20 levels makes NKFD less efficient than FPA. Using the linearized problem (**NKLP**) reduces the cost for Krylov evaluation significantly. The overall convergence rate is slightly decreased and it is again observed, that reuse of Krylov information (**NKLP-R**) reduces the number of Krylov iterations significantly (-55.8% for $\Delta t = 5.0e^{-4}\,[s]$ and -56.3% for $\Delta t = 10.0e^{-4}\,[s]$). Again, only a linear convergence rate of the overall problem can be reached and there still exists the cost of additional Krylov evaluation. It can be seen from the CPU time, that NKLP is much faster than NKFD and performs better than FPA. In this case, the linearization approach is able to represent decisive aspects of the coupled problem. The time step influence in both Newton Krylov schemes is less than in QN.

6.2 Problem FSI3

The resulting transient displacement of point A in x- and y-direction is shown in fig. 3. It can be seen, that after an inital phase the beam shows a harmonic oscillation with constant frequency and amplitude, which is the result of the interaction between Karmann vortices and beam deformation.

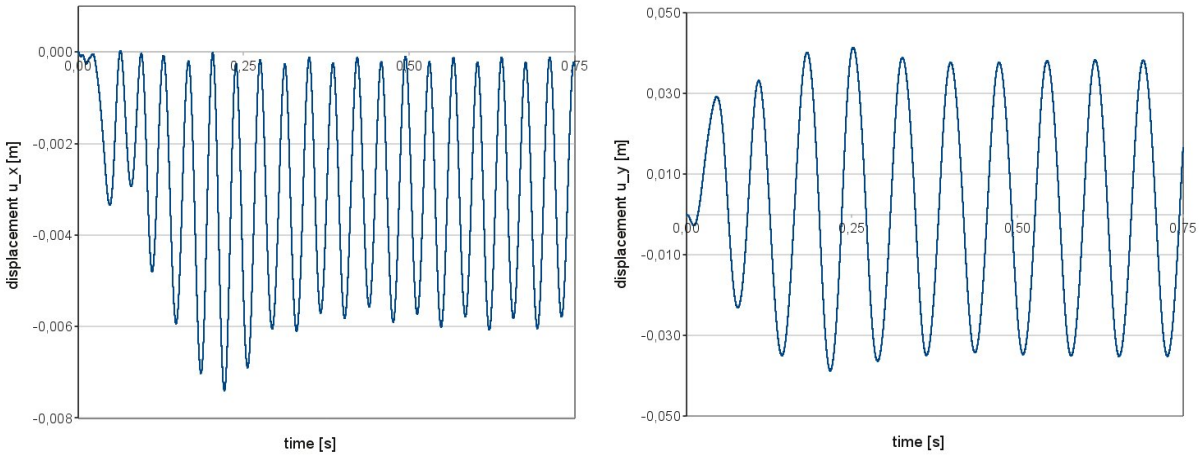

Figure 3: FSI3 - Displacement of Point A in x- and y-direction

In the following, the different coupling algorithms are used to compute the coupled system's behavior. The first 300 timesteps are computed. To compare w.r.t. efficiency, the average number of necessary coupling iterations and the relative computing time is given. To compare w.r.t. stability, two increasing time step sizes are examined, $\Delta t = 2.5e^{-4}\,[s]$, what corresponds to a maximum Courant number of 0.8, and $\Delta t = 10.0e^{-4}\,[s]$, what corresponds to a maximum Courant number of 3.2, in the undeformed fluid configuration. The results are summarized in table 3.

	$\Delta t = 0.00025$		$\Delta t = 0.001$	
	Iterations	CPU time	Iterations	CPU time
FPA	20.083	1.00	32.177	1.00
QN	10.253	0.54	12.983	0.41
QN-R(10)	6.567	0.34	7.690	0.28
QN-R(20)	6.460	0.33	8.257	0.26
NKFD	5.253 (33.76)	2.50	9.493 (67.64)	2.39
NKFD-R(10)	5.296 (24.62)	1.91	9.477 (45.333)	1.72
NKFD-R(20)	6.097 (18.990)	1.59	10.650 (36.473)	1.51
NKLP	11.927 (65.633)	1.33	12.917 (88.533)	0.84
NKLP-R(10)	11.953 (33.200)	0.96	13.023 (47.375)	0.60
NKLP-R(20)	11.857 (24.057)	0.88	13.010 (34.220)	0.54

Table 3: Comparison for FSI3

As the standard approach, Aitken's method (**FPA**) needs 20.083 iterations with $\Delta t = 2.5e^{-4}\,[s]$ and 32.177 iterations with $\Delta t = 10.0e^{-4}\,[s]$, so in this case a large time step influence is observed (+60.2% iterations). This is due o the greater nonlinearity of this case. The Quasi-Newton method in its basic version (**QN**) only needs 10.253 and 12.983 iterations, so a reduction by 48.9% and 59.7% is obtained. The time step influence in QN method is smaller than in FPA (+26.6% iterations). Reuse of history information (**QN-R**) gives an additional large increase in performance, with a low additional cost. Reusing 20 history levels (QN-R(20)) leads to 6.460 iterations with $\Delta t = 2.5e^{-4}\,[s]$ and a reduction by 37.0% and 8.257 iterations with $\Delta t = 10.0e^{-4}\,[s]$ and a reduction by 36.4% compared to QN. Newton-Krylov with Finite Differences (**NKFD**) needs 5.253 iterations for $\Delta t = 2.5e^{-4}\,[s]$. So in terms of coupling iterations only it needs less iterations than QN and FPA methods and gives approximately linear convergence rates. Reuse of Krylov information (**NKFD-R**) leads to a significant reduction of necessary GMRES iterations (-40.8% for $\Delta t = 2.5e^{-4}\,[s]$ and -46.1% for $\Delta t = 10.0e^{-4}\,[s]$). The huge additional cost of GMRES iterations can be seen from the CPU time. All NKFD methods need clearly more time then FPA and QN. It also has to be noted that the time step influence on NKFD is very large (+80.7% for $\Delta t = 2.5e^{-4}\,[s]$ and +76.7% for $\Delta t = 10.0e^{-4}\,[s]$) compared to QN. Using the linearized problem (**NKLP**) reduces the cost for one Krylov evaluation significantly. But due to the higher nonlinearity of this case, the evaluation quality of the linearized problem is not good, leading to a large increase in coupling and Krylov iterations ($\Delta t = 2.5e^{-4}\,[s]$: +127.1% coupling and +94.4% Krylov iterations for NKLP and +94.5% coupling and +20.3% Krylov iterations for NKLP-R(20), $\Delta t = 10.0e^{-4}\,[s]$: +36.1% coupling and +30.9% Krylov iterations for NKLP and +94.5% coupling and +20.3% Krylov iterations for NKLP-R(20)). Again, reuse of Krylov information reduces the number of Krylov iterations significantly (down by -63.3%). In this case, the linearization approach is not able to represent the decisive aspects of the coupled problem properly. To summarize, due to greater nonlinearity the total number

of coupling iterations is higher than in the case of FSI2. Only the NKFD method gives approximately linear convergence rates, but has the costly additional Krylov evaluation and is therefore not competitive. The linearized evaluation is not suitable in this case. Again, the Quasi-Newton method with reuse gives the best performance of all examined schemes.

6.3 Conclusion

The following conclusions can be drawn from these two examples:

- It is possible to reach a significant increase in performance compared to the standard Aitken method.
- The examined Quasi-Newton method is the most efficient one and allows the reuse of black-box field solvers.
- The examined Newton-Krylov methods need specific single field solution approaches, but do not yield to better performance than Quasi-Newton.
- In general, the reuse of history information leads to a large performance increase.
- Newton-Krylov and Quasi-Newton can give linear and QNR even superlinear convergence rates.
- The Krylov evaluation scheme is the decisive factor for the effectivity of Newton-Krylov schemes. This aspect is typically not mentioned in literature.
- Although large time steps are examined, none of the methods show stability problems.

7 Summary

In this paper different common algorithms for the partitioned solution of strongly coupled fluid-structure interaction problems are examined. The algorithms are compared w.r.t. efficiency and stability. It is shown, that the examined Quasi-Newton method is the most efficient and superlinear convergence can be reached. It also allows the use of black-box field solvers. The examined Newton-Krylov methods are less efficient. Additionally, they require the costly adaption of single field solvers, what is against the basic idea of partitioned schemes. Therefore, the Quasi-Newton method is prefered to other methods, because it allows the combination of efficiency and simplicity.

REFERENCES

[1] Chung, J. and Hulbert, G.M., A time integration algorithm for structural dynamics with improved numerical dissipation: The generalized-alpha Method, *Journal of Applied Mechanics*, **60**, 371-375 (1993).

[2] Newmark, N.M., A method of computation for structural dynamics, *Journal of the Engineering Mechanics Division*, **85**, 67-94 (1959).

[3] Tukovic, Z. and Jasak, H., Simulation of Free-Rising Bubble with Soluble Surfactant using Moving Mesh Finite Volume/Area Method, Proceddings of the *6th International Conference on CFD in Oil & Gas, Metallurgical and Process Industries* (2008).

[4] Demirdĉić, I. and Perić, M., Space conservation law in finite volume calculations of fluid flow, *International Journal for Numerical Methods in Fluids*, **8**, 1037-1050 (1988).

[5] Issa, R.I., Solution of the Implicitly Discretised Fluid Flow Equations by Operator-Splitting, *Journal of Computational Physics*, **62**, 40-65 (1985).

[6] Jasak, H., Error Analysis and Estimation for the Finite Volume Method with Applications to Fluid Flows, PhD thesis at *Imperial College London* (1996).

[7] Jasak, H. and Tukovic, Z., Automatic Mesh Motion for the Unstructured Finite Volume Method, *Transactions of FAMENA*, **30**, 1-18 (2007).

[8] Mok, D. P., Partitionierte Lösungsansätze in der Strukturdynamik und der Fluid-Struktur-Interaktion, PhD thesis at *Institut für Baustatik der Universität Stuttgart* (2001)

[9] Küttler, U. and Wall, W. A., Fixed-point fluid-structure interaction solvers with dynamic relaxation, *Computational Mechanics*, **43(1)**, 61-72 (2008).

[10] Küttler, U. and Wall, W., Vector extrapolation for strong coupling fluid-structure interaction solvers, *Journal of Applied Mechanics*, **76** (2009).

[11] Vierendeels, J., Lanoye, L., Degroote, J. and Verdonck, P., Implicit coupling of partitioned fluid-structure interaction problems with reduced order models, *Computers and Structures*, **85**, 970-976 (2007).

[12] Degroote, J., Bathe, K.-J. and Vierendeels, J., Performance of a new partitioned procedure versus a monolithic procedure in fluidstructure interaction, *Computers & Structures*, **87:11-12**, 793-801,(2009).

[13] Degroote, J., Annerel, S. and Vierendeels, J., Stability analysis of Gauss–Seidel iterations in a partitioned simulation of fluid-structure interaction, *Computers and Structures*, **88:5-6**, 263-271 (2010).

[14] Saad, Y. and Schultz, M.H., GMRES: A generalized minimal residual algorithm for solving nonsymmetric linear systems, *SIAM J. Sci. Stat. Comput.*, **7:3**, 856-869 (1986)

[15] van Brummelen, E.H., Michler, C. and de Borst, R., Interface-GMRES (R) acceleration of subiteration for fluid-structure-interaction problems, Technical Report DACS-05-001 at *Delft Aerospace Computational Science* (2005)

[16] Matthies, H.G. and Steindorf, J., Partitioned but strongly coupled iteration schemes for nonlinear fluid-structure interaction, *Computers and Structures*, **80:27-30**, 1991-1999 (2002)

[17] Matthies, H.G. and Steindorf, J., Partitioned strong coupling algorithms for fluid-structure interaction, *Computers and Structures*, **81:8-11**, 805-812 (2003)

[18] Michler, C., Van Brummelen, E.H. and De Borst, R., An interface Newton-Krylov solver for fluid-structure interaction, *International Journal for Numerical Methods in Fluids*, **47:10-11**, 1189-1195 (2005)

[19] Gerbeau, J.-F. and Vidrascu, M., A Quasi-Newton Algorithm Based on a Reduced Model for Fluid-Structure Interaction Problems in Blood Flows, *ESAIM: Math Model Numer Anal*, **37(4)**, 631-648 (2003)

[20] Gerbeau, J.F., Vidrascu, M. and Frey, P., Fluid-structure interaction in blood flows on geometries based on medical imaging, *Computers and Structures*, **83(2-3)**, 155-165 (2005)

[21] Deparis, S., Gerbeau, J.-F. and Vasseur, X., A Dynamic Preconditioner for Newton-Krylov Algorithms. Application to Fluid-Structure Interaction, *INRIA techreport* (2004)

[22] Turek, S. and Hron, J., Proposal for Numerical Benchmarking of Fluid-Structure Interaction between an Elastic Object and Laminar Incompressible Flow, *Lecture Notes in Computational Science and Engineering*, **53**, 371-385 (2006)

[23] International Workshop on Fluid-Structure Interaction - Theory, Numerics and Applications, Harmann, S., Meister, A., Schäfer, M. and Turek, S. Eds., kassel unviersity press (2009)

[24] Fluid-Structure Interaction. Part II, *Lecture Notes in Computational Science and Engineering*, Hans-Joachim Bungartz and Michael Schäfer Eds., 53, Springer (2010)